3, 6-Dithiophen-2-yl-diketopyrrolo [3, 2-b] pyrrole (isoDPPT) as an Acceptor Building Block for Organic Opto-Electronics

10 AUTHORS, INCLUDING:

Shaofeng Lu
Polyera Corporation
16 PUBLICATIONS   **415** CITATIONS

SEE PROFILE

Damien Boudinet
Polyera Corporation
20 PUBLICATIONS   **311** CITATIONS

SEE PROFILE

Yuning Li
University of Waterloo
129 PUBLICATIONS   **5,200** CITATIONS

SEE PROFILE

Hakan Usta
Abdullah Gül Üniversitesi
38 PUBLICATIONS   **1,636** CITATIONS

SEE PROFILE

3,6-Dithiophen-2-yl-diketopyrrolo[3,2-b]pyrrole (isoDPPT) as an Acceptor Building Block for Organic Opto-Electronics

Shaofeng Lu,[†,*] Martin Drees,[†] Yan Yao,[†] Damien Boudinet,[†] He Yan,[†] Hualong Pan,[†] Jingqi Wang,[†] Yuning Li,[‡] Hakan Usta,[†] and Antonio Facchetti[†,*]

[†]Polyera Corporation, 8045 Lamon Avenue, Skokie, Illinois 60077, United States

[‡]Department of Chemical Engineering and Waterloo Institute for Nanotechnology (WIN), University of Waterloo, 200 University Avenue West, Ontario, Canada, N2L 3G1

Ⓢ Supporting Information

ABSTRACT: The electron acceptor building block for π-conjugated copolymers, 3,6-dithiophen-2-yl-diketopyrrolo[3,2-b]-pyrrole (isoDPPT), was synthesized following two routes. The comparison between isoDPPT and widely investigated 3,6-dithiophen-2-yl-diketopyrrolo[3,4-c]pyrrole (DPPT) in terms of molecular orbital computations, single crystal X-ray diffraction, optical absorption and cyclic voltammogram was utilized to elucidate structural and electronic structure differences between the two cores. Both units are found to be planar in the solid state,

exhibit similar LUMO energy, however, isoDPPT exhibits a much deeper HOMO energy. Six isoDPPT-based polymers with optical bandgaps spanning from 1.44 to 1.76 eV were synthesized by copolymerizing isoDPPT with the following building blocks: 2,2′-bithiophene (for **P1**), 4,4′-bis(2-ethylhexyl)-dithieno[3,2-b:2′,3′-d]silole (for **P2**), 3,3′′′-didodecylquaterthiophene (for **P3**), 4,8-didodecylbenzo[1,2-b:4,5-b′]dithiophene (for **P4**), 4,8-didodecyloxybenzo[1,2-b:4,5-b′]dithiophene (for **P5**) and 3,3′-bis(dodecyloxy)-2,2′-bithiophene (for **P6**). Field-effect transistors and bulk heterojunction solar cells based on isoDPPT copolymers were fabricated and the response compared vis-a-vis to those of some DPPT-based polymers. Hole mobility (μ_h) of 0.03 cm²/(V·s) and solar cell power conversion efficiency (PCE) of 5.1% were achieved for polymer **P2**.
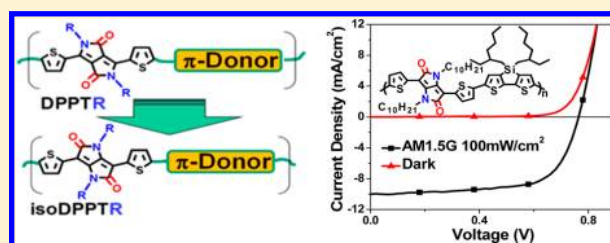
■ INTRODUCTION

The development of new π-conjugated building blocks is essential for deepening our understanding of organic semi-conductor chemistry[1] and microstructure versus charge transport[2] and possibly enabling their use in a variety of opto-electronic devices, such as organic thin film transistors (OTFTs),[3] organic photovoltaics (OPVs)[4] and organic light emitting diodes (OLEDs) and transistors (OLETs).[5] Starting from seminal studies on acenes[6] and simple oligo(poly)-heterocycles,[7] the field has moved to more elaborated structures comprising heterofused systems enabling impressive performance.[8]

Thus, during the past few years several organic semi-conductor classes have met basic criteria for organic electronics applications.[9] Among the most successful building blocks for semiconducting polymers, 3,6-dithiophen-2-yl-diketopyrrolo-[3,4-c]pyrrole (DPPT) has certainly attracted crescent attention.[10−12] First reported in 2008 by Winnewisser et al.,[10] 2-hexyldecyl substituted DPPT was coupled with two 3-dodecylthiophenes and then homopolymerized to give the polymer BBTDPP1 (Figure 1) and used as an ambipolar transporter in FETs exhibiting balanced hole and electron mobilites (μ) of ≈0.1 cm²/(V·s) and somehow a small $I_{on/off}$ ratio of ≈10². Very shortly after, Janssen et al. reported a similar copolymer (pBBTDPP2) affording a 4.0% power conversion efficiency (PCE) in combination with PC$_{71}$BM.[11] After these

reports, numerous DPPT-based polymers have been synthesized and utilized in both OTFT and OPV applications.[12] Via proper selection of the donor comonomers and extensive optimization of the semiconductor film microstructure and device fabrication, DPPT-based polymers are now among, if not the best materials for TFTs with unipolar hole mobilities exceeding 8 cm²/(V·s), unipolar electron mobilities in excess of 2 cm²/(V·s), and ambipolar mobility >1 cm²/(V·s),[12d−j] as well as exhibiting excellent OPV efficiencies of 5−6%.[12k−n] However, their impressive performance is typically achieved upon high temperature thermal annealing and/or under inert conditions. In addition to polymers, DPPT-based small molecules were also found to be active in OPVs[12b] and OTFTs.[13] For instance, DPP(TBFu)$_2$:PC$_{71}$BM devices were reported to achieve PCEs of 4.4 ± 0.4% with V_{oc} of 0.9 V[14a] while pyrene extended DPPs with PC$_{71}$BM gave PCE of up to 4.1%.[14b] When naphthodithiophene was end-functionalized with DPPT, its blend with PC$_{61}$BM resulted in PCE of 4.06 ± 0.06%.[14c] Recently, quinoidal TDPPT derivatives were reported as new n-type semiconductors with electron mobilities up to 0.55 cm²/(V·s).[13a]
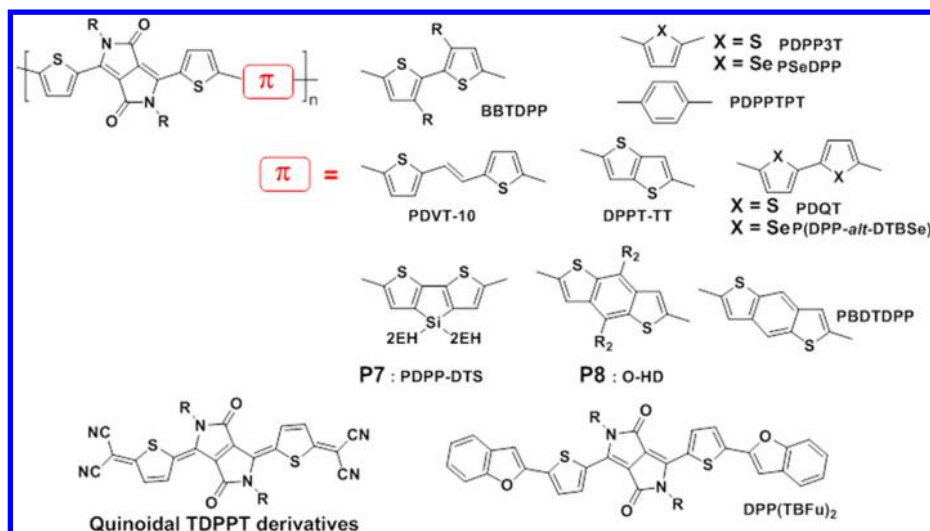
Figure 1. Chemical structure of some DPPT-based polymers, including **P7** and **P8** (vide infra), and small molecules.

It is well recognized that both the bandgap and molecular orbital energy levels of polymer donors should be optimized simultaneously to achieve high device performance for organic photovoltaics.[4] Structures with deep HOMO would enhance the open circuit voltage (V_{oc}), however, a delicate balance with the LUMO energy is necessary as not to compromise light absorption at longer wavelengths. As far as p-channel OTFTs are concerned, again a fine-tuning of the HOMO energy is needed to enable both good hole transport (typically optimized for high HOMO energy to match the work function of metal electrodes) and air stability (requiring low HOMO energy against ambient oxidation). With these needs in mind and considering the great interest of the DPPT structures, herein we report in details after our first discovery,[15a] the design, synthesis, and structural characterization of the acceptor building block 3,6-dithiophen-2-yl-diketopyrrolo[3,2-*b*]pyrrole (isoDPPT) following two complementary routes, a comparative study with the corresponding regioisomeric DPPT unit, and the initial investigation on OPV and TFT performance of several new donor−acceptor copolymers. Our results provide new fundamental information about the molecular structure of this core versus the corresponding DPP one, expand our understanding of their electronic structure difference, and provide new information about properties and performance of isoDPPT copolymers in opto-electronic devices versus very recent reports.[15b−d]

■ EXPERIMENTAL SECTION

Materials. All reagents were purchased from commercial sources and used without further purification unless otherwise noted. Of the comonomers, 5,5′-bis(trimethylstannyl)-2,2′-bithiophene was purchased from Sigma-Aldrich while 4,4′-bis(2-ethylhexyl)-5,5′-bis-(trimethylstannyl)-dithieno[3,2-*b*:2′,3′-*d*]silole,[16a] 5,5′″-bis-(trimethylstannyl)-3,3′″-didodecylquaterthiophene,[16b] 2,6-bis-(trimethylstannyl)-4,8-didodecylbenzo[1,2-*b*:4,5-*b*′]dithiophene,[16c] 2,6-bis(trimethylstannyl)-4,8-didodecyloxybenzo[1,2-*b*:4,5-*b*′]-dithiophene[16d] and 5,5′-bis(trimethylstannyl)-3,3′-bis(dodecyloxy)-2,2′-bithiophene[16e] were synthesized according to published procedures. DPPT2BO was also synthesized following the reported method.[14b] Anhydrous THF was distilled from Na/benzophenone. Conventional Schlenk techniques were used and reactions were carried out under N_2 unless otherwise noted.

Characterization. UV−vis spectra were recorded on a Cary 50 UV−vis spectrophotometer. NMR spectra were recorded on a Varian

Unity Plus 500 spectrometer (¹H, 500 MHz). Elemental analysis was done at Midwest Microlab, LLC. Molecular weight of polymers was determined by Cirrus GPC220 high temperature gel permeation chromatography at 150 °C with trichlorobenzene stabilized by 0.0125%BHT. Cyclic voltammetry measurement was carried out under nitrogen at a scan rate of 50 mV/s using a BAS-CV-50W voltammetric analyzer. A platinum disk working electrode, a platinum wire counter electrode and a silver wire reference electrode were employed and Fc/Fc⁺ (0.54 V vs SCE) was used as reference for all measurements. Single crystal of isoDPPTMe ($C_{16}H_{12}N_2O_2S_2$) was obtained from slow diffusion of methanol to the toluene solution, mounted in inert oil and transferred to the cold gas stream of a Bruker Kappa APEX2 CCD area detector equipped with a CuKα sealed tube with Quazar optics. SADABS-2008/1 (Bruker, 2008) was used for absorption correction. wR2(int) was 0.1160 before and 0.0578 after correction. The ratio of minimum to maximum transmission is 0.6753. The λ/2 correction factor is 0.0015.

Monomer Synthesis. *Ethyl 2-Thiopheneacetylaminoacetate (1).* To a suspension of glycine ethyl ester hydrochloride (21.77 g, 156 mmol) in anhydrous dichloromethane (260 mL) at 0 °C was added 1,8-diazabicyclo[5.4.0]undec-7-ene (55 mL, 368 mmol) under nitrogen and the suspension turned clear. Then 2-thiopheneacetyl chloride (19.2 mL, 156 mmol) was added dropwise. After completion of the addition, the flask was warmed to room temperature and the mixture was stirred for 1 h. Then it was washed with water (260 mL × 3), dried and concentrated. Dark brown oil was obtained (31.77 g, yield 89%), which turned into a dark brown solid upon standing. It is used directly for the next step without further purification. A light brown solid as the analytical sample was obtained by column chromatography with ethyl acetate as the eluent. ¹H NMR (CDCl₃, 500 MHz): δ = 7.26 (dd, J = 5.0, 1.0 Hz, 1H), 7.01−6.97 (m, 2H), 6.19 (s, 1H), 4.18 (q, J = 7.0 Hz, 2H), 4.00 (d, J = 5.0 Hz, 2H), 3.83 (s, 2H), 1.26 (t, J = 7.0 Hz, 3H). Anal. Calcd for $C_{10}H_{13}NO_3S$: C, 52.85; H, 5.77; N, 6.16. Found: C, 52.96; H, 5.80; N, 6.20.

3-Thiophen-2-yl-pyrrolidine-2,4-dione (2). To a solution of ethyl 2-thiopheneacetylaminoacetate (1) (31.77 g, 140 mmol) in anhydrous toluene (190 mL) was added potassium *tert*-butoxide (20.95 g, 187 mmol). The mixture was heated to reflux for 2 h. After cooling, it was poured into water (190 mL) and the water phase was isolated and acidified with dilute HCl to about pH 1 (~70 mL 10% HCl). The pale brown precipitate was filtered, washed with water and dried. Finally, a pale brown solid with some dark brown chunks was obtained (23.8 g, yield 94%) and used directly for the next step without further purification. ¹H NMR (DMSO-d_6, 500 MHz): δ = 7.55 (dd, J = 3.5, 1.0 Hz, 1H), 7.48 (s, 1H), 7.30 (dd, J = 5.0 1.0 Hz, 1H), 7.01 (dd, J = 5.0, 4.0 Hz, 1H), 3.88 (s, 2H). Anal. Calcd for $C_8H_7NO_2S$: C, 53.03; H, 3.89; N, 7.73. Found: C, 54.20; H, 4.34; N, 7.29.

4-Amino-3-thiophen-2-yl-1,5-dihydropyrrol-2-one (**3**). To a round-bottom flask with a Dean−Stark distilling receiver were charged ammonium acetate (20.90 g, 271 mmol) and xylene (215 mL), and the reaction was kept at 60 °C. Then 3-thiophen-2-yl-pyrrolidine-2,4-dione (**2**) (19.0 g, 105 mmol) was added portionwise. The mixture was heated to reflux until there was no more water collected by the receiver (about 15 mL water), and a sticky gel was formed at the bottom. After cooling, toluene was decanted, and the sticky gel was further washed by toluene and water and dried under vacuum at 80 °C. Finally, a sticky gel was obtained (18.3 g, yield 97%), which can be used directly for the next step. A yellowish solid as the analytical sample was obtained by cooling down the hot toluene solution slowly and then filtration. ^{1}H NMR (DMSO-d_6, 500 MHz): δ = 7.23 (s, 1H), 7.22 (s, 1H), 7.10 (s, 1H), 7.00 (dd, J = 5.0, 4.0 Hz, 1H), 6.77 (s, 2H), 3.82 (s, 2H). Anal. Calcd for $C_8H_8N_2OS$: C, 53.32; H, 4.47; N, 15.54. Found: C, 53.28; H, 4.61; N, 14.82.

3,6-Dithiophen-2-yl-diketopyrrolo[3,2-b]pyrrole (**4**). To a round-bottom flask with the sticky gel product (**3**) obtained above were added amyl alcohol (254 mL) and *t*-BuOK (11.4 g, 102 mmol), and the mixture was heated to reflux until the viscosity of the mixture lowered to allow stirring (~10 min). A solution of ethyl thiophene-2-glyoxylate (15 mL, 102 mmol) in amyl alcohol (15 mL) was added dropwise in 3 h and the reaction mixture was heated to reflux for 14 h. After cooling, the reaction mixture was diluted with MeOH (305 mL), neutralized with HOAc (7 mL), filtered, and washed with MeOH (250 mL × 2) and water (250 mL). The solid was dried under vacuum at 80 °C for 2 days. Finally, a mixture of 3,6-dithiophen-2-yl-diketopyrrolo-[3,2-b]pyrrole (**4**) and unreacted 4-amino-3-thiophen-2-yl- 1,5-dihydropyrrol-2-one (**3**) with the molar ratio of about 1:1 was obtained (17.66 g). An orange solid as the analytical sample was obtained by using the analytical 4-amino-3-thiophen-2-yl-1,5-dihydropyrrol-2-one (**3**) as the starting material instead of the crude. ^{1}H NMR (DMSO-d_6, 500 MHz): δ = 11.12 (s, 2H), 7.65 (d, J = 5.0 Hz, 2H), 7.62 (d, J = 4.0 Hz, 2H), 7.18 (dd, J = 5.0, 4.0 Hz, 2H). Anal. Calcd for $C_{14}H_8N_2O_2S_2$: C, 55.99; H, 2.68; N, 9.33. Found: C, 55.62; H, 2.97; N, 8.91.

1,4-Bis(2-butyloctyl)-3,6-dithiophen-2-yl-diketopyrrolo[3,2-b]-pyrrole (isoDPPT2BO). To a round-bottom flask under nitrogen were added 3,6-dithiophen-2-yl-diketopyrrolo[3,2-b]pyrrole (the 1:1 mixture of **3** and **4**, 1.8 g, 6 mmol), Cs_2CO_3 (4.89 g, 15 mmol) and anhydrous DMF (60 mL), and the reaction was stirred at 60 °C. 2-Butyloctyl iodide (3.0 mL, 12 mmol) was added in one portion and the reaction mixture was kept at 60 °C for 24 h. After removing the solvent, chloroform (30 mL) was added and the mixture was stirred for 10 min before it was filtered through coarse Celite diatomaceous earth particles. After concentration, the crude was purified by a short column with a 3:1 mixture of chloroform:hexane as the eluent to give an orange solid (500 mg, yield 13%). ^{1}H NMR (CDCl$_3$, 500 MHz): δ = 7.62 (d, J = 5.0 Hz, 2H), 7.30 (d, J = 3.5 Hz, 2H), 7.13 (dd, J = 5.0, 3.5 Hz, 2H), 3.74 (d, J = 7.5 Hz, 4H), 1.40−1.00 (m, 38H), 0.87 (t, J = 7.5 Hz, 6H), 0.83 (t, J = 7.0 Hz, 6H). Anal. Calcd for $C_{38}H_{56}N_2O_2S_2$: C, 71.65; H, 8.86; N, 4.40. Found: C, 71.68; H, 8.69, N; 4.42. Mp 106−108 °C.

1,4-Bisdecyl-3,6-dithiophen-2-yl-diketopyrrolo[3,2-b]pyrrole (isoDPPTDec). To a round-bottom flask under nitrogen were added 3,6-dithiophen-2-yl-diketopyrrolo[3,2-b]pyrrole (the 1:1 mixture of **3** and **4**, 1.8 g, 6 mmol), Cs_2CO_3 (4.89 g, 15 mmol) and anhydrous DMF (60 mL), and the recation was stirred at 120 °C. Decyl bromide (3.1 mL, 15 mmol) was added in one portion, and the reaction mixture was kept at 60 °C for 24 h. After removing the solvent, chloroform (50 mL) was added and the mixture was stirred for 10 min before it was filtered through coarse Celite diatomaceous earth particles. After concentration, the crude was purified by a short column with chloroform as the eluent to give an orange solid (739 mg, yield 23%). ^{1}H NMR (CDCl$_3$, 500 MHz): δ = 7.44 (d, J = 5.0 Hz, 2H), 7.37 (d, J = 3.5 Hz, 2H), 7.13 (dd, J = 5.0, 3.5 Hz, 2H), 3.83 (t, J = 7.5 Hz, 4H), 1.46−1.37 (m, 4H), 1.32−1.14 (m, 28H), 0.88 (t, J = 7.0 Hz, 6H). Anal. Calcd for $C_{34}H_{48}N_2O_2S_2$: C, 70.30; H, 8.33; N, 4.82. Found: C, 70.28; H, 8.45; N, 4.78.

1,4-Dimethyl-3,6-dithiophen-2-yl-diketopyrrolo[3,2-b]pyrrole (isoDPPTMe). To a pressure reactor under nitrogen were added 3,6-dithiophen-2-yl-diketopyrrolo[3,2-b]pyrrole (the 1:1 mixture of **3** and **4**, 1.8 g, 6 mmol), Cs_2CO_3 (4.89 g, 15 mmol), anhydrous DMF (40 mL), and iodomethane (1.87 mL, 30 mmol). The reactor was sealed and the reaction mixture was kept at 110 °C for 24 h. After cooling down and removing the solvent, chloroform (50 mL) was added and the mixture was stirred for 10 min before it was filtered through coarse Celite diatomaceous earth particles. After concentration, the crude was purified by a short column with chloroform as the eluent to give a red solid (308 mg, yield 18%). ^{1}H NMR (CDCl$_3$, 500 MHz): δ = 7.46 (d, J = 3.5 Hz, 2H), 7.44 (d, J = 5.0 Hz, 2H), 7.13 (dd, J = 5.0, 3.5 Hz, 2H), 3.39 (s, 6H). The single crystal of isoDPPT-Me was then grown by slow diffusion of methanol to its toluene solution and subjected to X-ray crystallography.

3,6-Bis(5-bromothiophen-2-yl)-1,4-bis(2-butyloctyl)-diketopyrrolo[3,2-b]pyrrole (isoDPPT2BO-Br2). To a round-bottom flask in the dark were added 1,4-bis(2-butyloctyl)-3,6-dithiophen-2-yl-diketopyrrolo[3,2-b]pyrrole (520 mg, 0.82 mmol), CHCl$_3$ (15 mL) and NBS (526 mg, 2.96 mmol). The mixture was stirred at room temperature for 24 h and concentrated to be purified by column chromatograph with a 2:1 mixture of CHCl$_3$:hexane as the eluent to give an orange solid (473 mg, yield 73%). ^{1}H NMR (CDCl$_3$, 500 MHz): δ = 7.06 (d, J = 4.0 Hz, 2H), 7.00 (d, J = 4.0 Hz, 2H), 3.67 (d, J = 7.5 Hz, 4H), 1.39−1.32 (m, 2H), 1.30−1.02 (m, 36H), 0.86 (t, J = 7.5 Hz, 6H), 0.82 (t, J = 7.0 Hz, 6H). Anal. Calcd for $C_{38}H_{54}Br_2N_2O_2S_2$: C, 57.43; H, 6.85; N, 3.52. Found: C, 57.52; H, 6.76; N, 3.47.

3,6-Bis(5-bromo-thiophen-2-yl)-1,4-bisdecyldiketopyrrolo[3,2-b]-pyrrole (isoDPPTDec-Br2). To a round-bottom flask in the dark were added 1,4-bisdecyl-3,6-dithiophen-2-yl-diketopyrrolo[3,2-b]pyrrole (793 mg, 1.36 mmol), CHCl$_3$ (25 mL), and NBS (875 mg, 4.92 mmol). The mixture was stirred at room temperature for 48 h and concentrated to be purified by column chromatograph with a 3:1 mixture of CHCl$_3$:hexane as the eluent to give an orange solid (863 mg, yield 86%). ^{1}H NMR (CDCl$_3$, 500 MHz): δ = 7.10−7.07 (m, 4H), 3.79 (t, J = 7.5 Hz, 4H), 1.50−1.40 (m, 4H), 1.34−1.14 (m, 28H), 0.89 (t, J = 7.0 Hz, 6H). Anal. Calcd for $C_{34}H_{46}Br_2N_2O_2S_2$: C, 55.28; H, 6.28; N, 3.79. Found: C, 55.29; H, 6.18; N, 3.75.

*N,N′-Dihexyloxalamide (**6**).[16f]* To a solution of hexylamine (13.3 mL, 100 mmol) in toluene (25 mL) with vigorous stirring at room temperature was added dropwise a solution of oxalyl chloride (2.2 mL, 25 mmol) in toluene (12 mL). After the addition, the mixture was heated to 60 °C for overnight. After cooling down, the mixture was concentrated, washed with hot water (50 mL X 2), redissolved in dichloromethane and dried over Na_2SO_4. After filtration, the solution was concentrated to give a white solid which was recrystallized from propylene carbonate (160 mL). After recrystallization, the solid was further washed with hot water (40 mL X 3 and then 200 mL), redissolved in dichloromethane, dried over Na_2SO_4 and concentrated to give N,N′-dihexyloxalamide as a white solid (6.4 g, yield 100%). Mp 130−132 °C. ^{1}H NMR (CDCl$_3$, 500 MHz): δ = 7.49 (br s, 2H), 3.34−3.29 (m, 4H), 1.60−1.52 (m, 4H), 1.40−1.24 (m, 12H), 0.90 (t, J = 7.0 Hz, 6H). Anal. Calcd for $C_{14}H_{28}N_2O_2$: C, 65.59; H, 11.01; N, 10.93. Found: C, 65.70; H, 10.88; N, 11.10.

*N,N′-Dihexyloxalimide dichloride (**7**).[16f]* A mixture of N,N′-dihexyloxalamide (**6**) (1.28 g, 5 mmol) and phosphorus pentachloride (2.08 g, 10 mmol) in toluene (20 mL) was refluxed for 6 h. After cooling down, the mixture was removed under reduced pressure. The resulting brown oil was used directly without further purification. ^{1}H NMR (CDCl$_3$, 500 MHz): δ = 3.73 (t, J = 7.5 Hz, 4H), 1.78−1.71 (m, 4H), 1.48−1.32 (m, 12H), 0.92 (t, J = 7.0 Hz, 6H).

1,4-Bishexyl-3,6-dithiophen-2-yl-diketopyrrolo[3,2-b]pyrrole (isoDPPTHex). To a solution of diisopropylamine (2.03 mL, 14.5 mmol) in THF (10 mL) under nitrogen at 0 °C was added dropwise *n*-butyllithium (5.3 mL, 13.2 mmom, 2.5 M in hexane). After 30 min, a solution of ethyl 2-thiopheneacetate (1.65 mL, 11 mmol) in THF (30 mL) was added dropwise. After 1 h stirring at 0 °C, the flask was cooled down to −78 °C and a solution of N,N′-dihexyloxalimide dichloride (**7**) (5 mmol) in THF (30 mL) was added dropwise. After

addition, the mixture was warmed to room temperature during 14 h and was stirred for 36 h more. The mixture was poured into saturated NH$_4$Cl solution and the organic phase was separated. The aqueous phase was extracted with CHCl$_3$ for several times. The organic extracts were combined, dried over Na$_2$SO$_4$, concentrated and purified by column chromatography with CHCl$_3$ as the eluent. Finally, an orange solid was obtained (235 mg, yield 10%). ^{1}H NMR (CDCl$_3$, 500 MHz): δ = 7.45 (d, J = 5.0 Hz, 2H), 7.40 (d, J = 3.5 Hz, 2H), 7.15 (dd, J = 5.0, 3.5 Hz, 2H), 3.85 (t, J = 7.5 Hz, 4H), 1.48−1.38 (m, 4H), 1.33−1.14 (m, 12H), 0.89 (t, J = 7.0 Hz, 6H). Anal. Calcd for C$_{26}$H$_{32}$N$_2$O$_2$S$_2$: C, 66.63; H, 6.88; N, 5.98. Found: C, 66.79; H, 6.69; N, 6.04.

Polymer Synthesis. *Preparation of P1.* In a 10 mL microwave tube, 5,5′-bis(trimethylstannyl)-2,2′-bithiophene (29.5 mg, 60 μmol), 3,6-bis(5-bromo-thiophen-2-yl)-1,4-bis(2-butyloctyl)diketopyrrolo-[3,2-b]pyrrole (47.7 mg, 60 μmol), Pd$_2$(dba)$_3$ (2.7 mg, 5 mol %), and tri(o-tolyl)phosphine (3.7 mg, 20 mol %) were mixed in anhydrous toluene (5 mL) under argon. Then the tube was heated to 180 °C in 30 min and kept at this temperature for 270 min by a CEM Discover Microwave reactor. After cooling, it was poured into MeOH (50 mL), filtered, and dried in a vacuum oven to give a black solid (44.0 mg, yield 92%). The crude has too little solubility for further purification. Anal. Calcd: C, 69.13; H, 7.31; N, 3.51. Found: C, 69.17, H, 7.22; N, 3.64.

Preparation of P2. In a 10 mL microwave tube, 4,4′-bis(2-ethylhexyl)-5,5′-bis(trimethylstannyl)dithieno[3,2-b:2′,3′-d]silole (43.82 mg, 60 μmol), 3,6-bis(5-bromothiophen-2-yl)-1,4-bisdecyldiketopyrrolo[3,2-b]pyrrole (44.44 mg, 60 μmol), Pd$_2$(dba)$_3$ (2.7 mg, 5 mol %), and tri(o-tolyl)phosphine (3.7 mg, 20 mol %) were mixed in anhydrous toluene (5 mL) under argon. Then the tube was heated to 180 °C in 30 min and kept at this temperature for 270 min by a CEM Discover Microwave reactor. After cooling, it was poured into MeOH (50 mL) and filtered. Using a Soxhlet setup, the crude product was extracted successively with MeOH, hexane, ethyl acetate and chloroform. The chloroform extract was poured into MeOH (100 mL) and the solid was collected. Finally, a black solid (31.1 mg, yield 52%, M_w = 31.4 kDa, d = 1.49) was obtained. Anal. Calcd: C, 69.97; H, 8.30; N, 2.81. Found: C, 69.61, H, 8.19; N, 2.86.

Preparation of P3. In a 100 mL storage vessel, 5,5‴-bis-(trimethylstannyl)-3,3‴-didodecylquaterthiophene (59.6 mg, 60 μmol), 3,6-bis(5-bromo-thiophen-2-yl)-1,4-bis(2-butyloctyl)-diketopyrrolo[3,2-b]pyrrole (47.7 mg, 60 μmol), Pd$_2$(dba)$_3$ (2.7 mg, 5 mol %), and tri(o-tolyl)phosphine (3.7 mg, 20 mol %) were mixed in anhydrous toluene (8 mL) under argon. Then the vessel was kept at 130 °C for 44 h. After cooling, the reaction mixture was poured into MeOH (50 mL), filtered, and dried in a vacuum oven to give a black solid. Using a Soxhlet setup, the crude product was extracted successively with MeOH, hexane, AcOEt, THF and CHCl$_3$. The CHCl$_3$ extract was poured into MeOH (100 mL) and the solid was collected. Finally, a black solid was obtained (60.2 mg, yield 77%, M_w = 91.9 kDa, d = 2.77). Anal. Calcd: C, 72.06; H, 8.53; N, 2.15. Found: C, 71.52, H, 8.21; N, 2.39.

Preparation of P4. In a 10 mL microwave tube, 2,6-bis-(trimethylstannyl)-4,8-didodecylbenzo[1,2-b:4,5-b']dithiophene (51.2 mg, 60 μmol), 3,6-bis(5-bromo-thiophen-2-yl)-1,4-bis(2-butyloctyl)-diketopyrrolo[3,2-b]pyrrole (47.7 mg, 60 μmol), Pd$_2$(dba)$_3$ (2.7 mg, 5 mol %), and tri(o-tolyl)phosphine (3.7 mg, 20 mol %) were mixed in anhydrous toluene (5 mL) under argon. Then the tube was heated to 180 °C in 30 min and kept at this temperature for 270 min by a CEM Discover Microwave reactor. After cooling, it was poured into MeOH (50 mL), filtered and dried in a vacuum oven to give a dark brown solid (68.4 mg). Using a Soxhlet setup, the crude product was extracted successively, with MeOH, hexane, ethyl acetate, THF, and chloroform. The chloroform extract was poured into MeOH (100 mL) and the solid was collected. Finally, a dark brown solid (62.1 mg, yield 89%, M_w = 61.9 kDa, d = 2.38) was obtained. Anal. Calcd: C, 74.56; H, 9.21; N, 2.42. Found: C, 74.42, H, 9.18; N, 2.55.

Preparation of P5. In a 10 mL microwave tube, 2,6-bis-(trimethylstannyl)-4,8-didodecyloxybenzo[1,2-b:4,5-b']dithiophene (53.1 mg, 60 μmol), 3,6-bis(5-bromo-thiophen-2-yl)-1,4-bis(2-

butyloctyl)diketopyrrolo[3,2-b]pyrrole (47.7 mg, 60 μmol), Pd$_2$(dba)$_3$ (2.7 mg, 5 mol %) and tri(o-tolyl)phosphine (3.7 mg, 20 mol %) were mixed in anhydrous toluene (5 mL) under argon. Then the tube was heated to 180 °C in 30 min and kept at this temperature for 270 min by a CEM Discover Microwave reactor. After cooling, it was poured into MeOH (50 mL), filtered, and dried in a vacuum oven to give a dark brown solid. Using a Soxhlet setup, the crude product was extracted successively with MeOH, hexane, ethyl acetate, ether and dichloromethane. The dichloromethane extract was poured into MeOH (100 mL) and the solid was collected. Finally, a dark brown solid (45.0 mg, yield 63%, M_w = 53.6 kDa, d = 1.85) was obtained. Anal. Calcd: C, 72.55; H, 8.96; N, 2.35. Found: C, 72.28, H, 8.85; N, 2.48.

Preparation of P6. In a 10 mL microwave tube, 5,5′-bis-(trimethylstannyl)-3,3′-didodecyloxy-2,2′-bithiophene (51.6 mg, 60 μmol), 3,6-Bis(5-bromo-thiophen-2-yl)-1,4-bis(2-butyloctyl)-diketopyrrolo[3,2-b]pyrrole (47.7 mg, 60 μmol), Pd$_2$(dba)$_3$ (2.7 mg, 5 mol %), and tri(o-tolyl)phosphine (3.7 mg, 20 mol %) were mixed in anhydrous toluene (5 mL) under argon. Then the tube was heated to 180 °C in 30 min and kept at this temperature for 270 min by a CEM Discover Microwave reactor. After cooling, it was poured into MeOH (50 mL), filtered, and dried in a vacuum oven to give a dark blue solid (66.1 mg). Using a Soxhlet setup, the crude product was extracted successively with MeOH, hexane, ethyl acetate, and THF. The THF extract was poured into MeOH (100 mL) and the solid was collected. Finally, a dark blue solid (55.5 mg, yield 79%, M_w = 47.9 kDa, d = 1.99) was obtained. Anal. Calcd: C, 71.99; H, 9.15; N, 2.40. Found: C, 71.74, H, 9.10; N, 2.54.

■ RESULTS AND DISCUSSION

In the following sections, we first report DFT computations comparing vis-a-vis the electronic structures and molecular orbital energies of the two isomeric diketopyrrolopyrrole DPP/isoDPP and DPPTMe/isoDPPTMe cores. Furthermore, we compare and discuss the crystal structures of two DPPT derivatives and that of isoDPPTMe. Both computation and single crystal analysis indicate that the electronic structure difference between these two regioisomeric deketopyrrolopyr-roles is intrinsic to the core atomic arrangement and not the result of the conjugation efficiency with the thiophene pendants (core planarity). Next, we report synthetic details for the isoDPPT monomers as well as the copolymerization of N,N'-dialkylated isoDPPT-Br$_2$ derivatives with six typical donor building blocks followed by the investigation on their optical and electrochemical properties. At the end, we report the initial application of these copolymers in field-effect transistors and bulk-heterojunction solar cells followed by a conclusion paragraph.

Molecular Orbital Computation and Single Crystal Analysis. This study initiated with molecular orbital (MO) calculations[17] (B3LYP/6-31G*) to compare the electronic structure and HOMO/LUMO energy levels of DPPTR and isoDPPTR (R = Me) (Figure 2, parts A and B).[18] After MO optimization, DPPTMe is found to be strictly planar while isoDPPTMe is twisted with a torsional angle of ≈24° between the thiophene pendant and the pyrrolinone ring. It is known that the carbonyl oxygens in DPPT form hydrogen bonds with the β-hydrogens of the adjacent thiophenes which strengthen core coplanarity[9] and promote self-assembly of DPPT-based polymers but greatly reduces the solution processability window.

The computed bond lengths on the central DPP/isoDPP 1,4-(dithien-2-yl)-buta-1,3-diene backbones and of those connecting these unit to the thienyl substituents are instructive to analyze since the bond length alternation can be regarded as
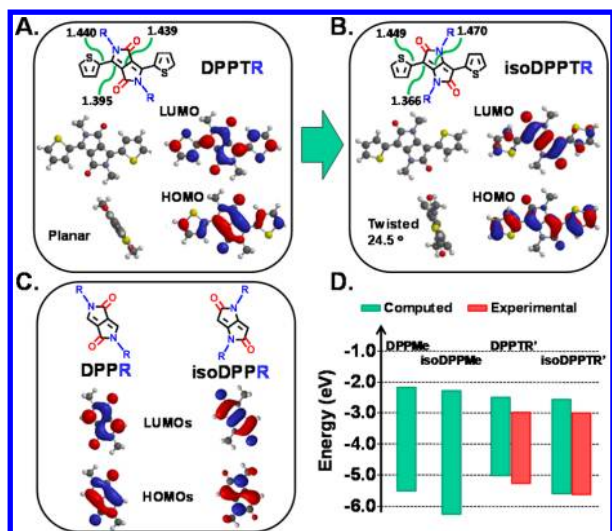
Figure 2. Chemical structure of DPPTR (A; R = Me), isoDPPTR (B; R = Me), and DPPR and isoDPPR (C; R = Me) as well as pictorial representations of the B3LYP-6-31G*-derived HOMO and LUMO orbitals. All bond lengths are in angstroms. (D) Corresponding energy level diagram.

an indicator of π-delocalization and, if present, aromaticity of the (hetero)aromatic units composing the molecule. As shown in Figure 2, parts A and B, DPPTMe has much closer bond lengths between the formal single and double bonds than isoDPPTMe. This could be explained by a more efficient π-conjugation between the thiophene rings with the central fused heterocycle in DPPTMe than in regioisomeric isoDPPTMe, suggesting a greater contribution of the quinoid character for the former isomer to the definition of the resonance structure. The computed HOMO/LUMO energies of isoDPPTMe and DPPTMe were found to be −5.65/−2.61 eV and −4.97/−2.51 eV, giving a bandgap of 3.04 and 2.46 eV, respectively. While the LUMO energies of the two systems are comparable, the HOMO of isoDPPTMe is substantially lower by ~0.68 eV, which could result in copolymers with deeper HOMOs as well as larger optical bandgaps (vide infra). The computed frontier molecular orbital (FMO) topologies for the two cores are also shown in Figure 2, parts A and B. From a qualitative analysis of the FMO topologies of the central unit it appears that both HOMO and LUMO are delocalized on more atoms for DPPTMe versus isoDPPMe. Strong localization is particularly severe for the HOMO of the isoDPP derivative which combined with the fact that the amide nitrogen has marginal participation in the MO wave function, may explain the associated deep energy level. Furthermore, this may suggest that N-substitution on isoDPPT will affect the orbital energy level even less than the corresponding DPPT-based derivatives.

To compare the two isomeric structures even more closely and rationalize whether the computed widening of the band gap in isoDPPT is only the result of reduced core planarity ($\approx24°$ twist angle for thiophene-isoDPP), MO calculations were also carried out on the unsubstitured DPPMe and isoDPPMe cores (Figure 2C). As expected, because of the anellation and negligible steric substitution, both isomers are planar. The FMO topological analysis evidences that both isoDPPMe and DPPMe HOMO and LUMO patterns resemble those of the thienyl-substituted cores, with minimal contribution from the N-Me nitrogen and C=O carbon atoms to the HOMO and LUMO wave functions, respectively. Thus,

DPPMe/isoDPPMe LUMO energies (−2.17/−2.36 eV) are far closer than the HOMO energies (−5.52/−6.29 eV), resulting in a far larger bandgap for isoDPPMe (3.93 eV) than for DPPMe (3.35 eV) (Figure 2D). Thus, the deeper HOMO and larger bandgap of isoDPPT-based derivatives, compared to the corresponding DPPTs, mostly originate from the intrinsic electronic structure and core atom connectivity of the isoDPP unit.

Recently, a very instructive study from Patil et al reported the single crystal structure of several DPPT derivatives functionalized with different alkyl groups on the nitrogen atoms, including hexyl (DPPTHex) and triethylene glycol mono methyl ether (DPPTEG) (Figure 3, parts A and B).[19] The solid
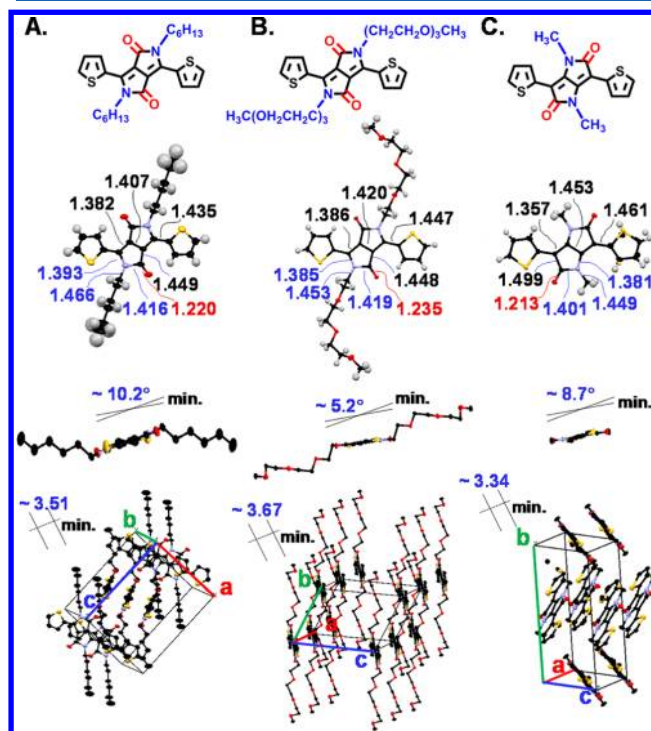

Figure 3. Chemical (top) and crystal structure from different views (bottom) of DPPTHex (A), DPPTEG (B), and isoDPPTMe (C). All bond lengths are in angstroms.

state packing and structures of these DPPT derivatives were thoroughly investigated indicating the existence of considerable $\pi-\pi$ stacking. To our knowledge, no structural analysis has ever been carried out for isoDPPT. Single crystals of isoDPPTMe were prepared by slow diffusion of methanol into a toluene solution and the crystal structure was determined by X-ray diffraction (Figure 3C). The details of data collection and refinement are given in the Supporting Information. IsoDPPTMe crystallizes in a monoclinic unit cell with a $P2_1/c$ space group. While the thiophene rings exhibit an *anti* conformation in DPPTHex and DPPTEG, in isoDPPTMe there is clear evidence of conformational *syn-anti* disorder for the thienyl substituents. This is the result of two different intramolecular interactions in isoDPPTMe, one between the carbonyl oxygen and the thiophene sulfur (C=O···S) being 2.800 Å and the other between the carbonyl oxygen and the hydrogen atom of the thiophene (C=O···H) at 2.366 Å. Both distances are shorter than the corresponding van der Waals distances for O···S (3.32 Å) and O···H (2.72 Å). The comparison between the crystal structures of DPPTHex

Scheme 1. Synthesis of isoDPPTR Derivatives by (A) Stepwise Cyclization and (B) One Pot Double Cyclization
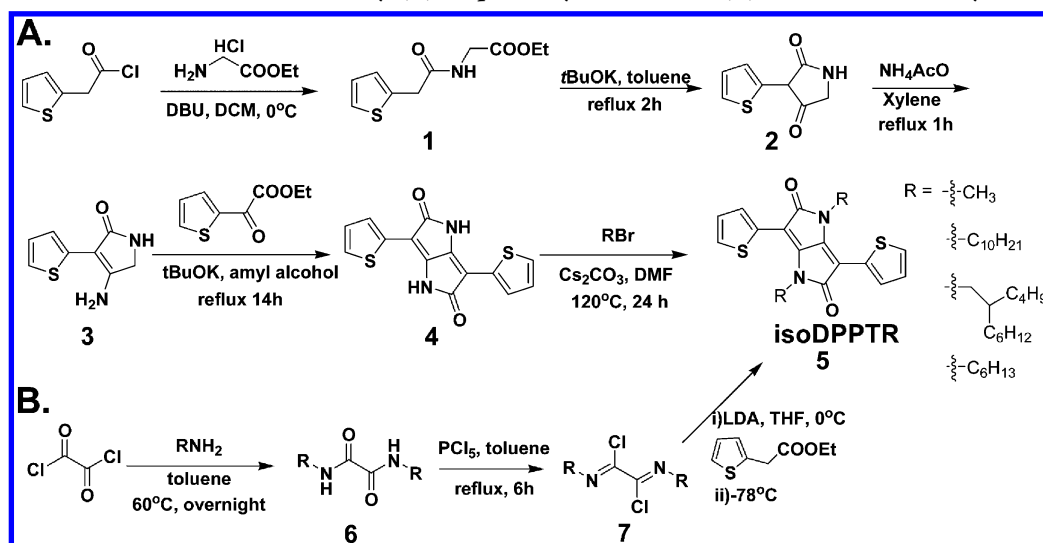
(Figure 3A) and DPPTEG (Figure 3B) with that of isoDPPTMe (Figure 3C) provides further insights into how isomerism affects core planarity, bond lengths, and packing characteristics of these derivatives. The crystal structure shows that all systems exhibit a brick-like packing with the molecules stacking, to different extents, the thiophene ring of one molecule with the anellated core of the adjacent one. Very interestingly, compared to the optimized computed structure, the isoDPPT core exhibits a rather planar solid state conformation with the torsional angle between the thiophene units and the isoDPP core being 8.7° (~16° smaller than the computation results). This is in contrast to the DPPT derivatives where the actual torsional angles were found much larger than the computed values (1.9°), being 10.2° for DPPTHex and 5.2° for DPPTEG, respectively.[19] The torsional angle variations between computed and X-ray geometries are the result of the different gas-phase versus condense phase environment for these methodologies, respectively. Figure 3 also shows selected bond lengths of the three compounds which confirm that the bond length alternation of isoDPPT is much larger than that of the DPPT derivatives. Indeed, the bonds involved in the conjugation between the thiophene substituents in isoDPPTMe vary from 1.357 to 1.499 Å with a difference of 0.142 Å. Note that this bond length variation is more than twice those found for DPPTHex (0.067 Å) and DPPTEG (0.063 Å), indicating that the conjugation through the isoDPP core is less efficient (more localization) than in DPP, which is consistent with the computational results. On the other hand, analysis of the solid state packing indicates that the core−core intermolecular distances are smaller in isoDPPTMe (~3.34 Å) than in both DPPTHex (~3.51 Å) and DPPTEG (~3.67 Å). Although the methyl substituent of the isoDPPT is less sterically demanding that a hexyl or TEG chain, this result likely suggests that intermolecular charge hopping efficiency should be equally favorable for the π-conjugated systems based in these isomeric cores. This conclusion obviously assumes that other energetic, morphological, and microstructural parameters are also equally favorable for charge transport.

Synthesis of isoDPPTR Building Blocks and Polymers. Given the interesting results from calculations and structural characterization, we approached the synthesis of the isoDPPT[15]

core based on known methodologies for other diketopyrrolo-[3,2-*b*]pyrroles. The isoDPP core could be synthesized in three different ways, namely stepwise cyclization starting from 2-(2-phenylacetamido)acetic esters,[20] one step from pulvinic acid[21] and one-pot double-cyclization of oxalic acid-bis(imidoyl) dichlorides.[22] Among them, stepwise cyclization allows one first to build the core and then introduce the amide alkyl chains. Furthermore, this route gives the possibility to prepare nonsymmetrical isoDPPT derivatives. On the other hand, the new one pot double cyclization allows faster access to the *N,N'*-disubstituted building blocks. Once the substitutions are selected through preliminary investigation of their effects on the polymer properties, the latter route after optimization could reduce synthetic costs due to less reaction steps, shorter reaction time, and easily accessible chemicals.

Here, the synthesis of isoDPPT was carried out following the two different routes shown in Scheme 1. Ethyl 2-thiophenea-cetylaminoacetate (**1**) was obtained in 89% yield by mixing glycine ethyl ester hydrochloride with 2-thiopheneacetyl chloride in the solution of 1,8-diazabicyclo[5.4.0]undec-7-ene (DBU) in CH_2Cl_2. Refluxing **1** in toluene with *t*-BuOK gave 3-thiophen-2-yl-pyrrolidine-2,4-dione (**2**) in 94% yield after acidification. Then ammonium acetate was combined with **2** for refluxing in xylene to quantitatively yield 4-amino-3-thiophen-2-yl-1,5-dihydropyrrol-2-one (**3**) as a gel which was directly mixed with *t*-BuOK and ethyl thiophene-2-gloxylate in refluxing amyl alcohol to result in a 1:1 mixture of **3** and 3,6-dithiophen-2-yl-diketopyrrolo[3,2-*b*]pyrrole (**4**). Further alkylation of the mixture with alkyl iodide or bromide gave the final product isoDPPTR (**5**). One-pot double-cyclization of oxaldi-(alkylimidoyl) dichloride was also attempted for *N,N'*-alkylated isoDPPTR since so far only (hetero)aryl oxaldiimidoyl dichlorides have been reported for successful cyclization.[15b] Alkylamine was mixed with oxalyl chloride to give *N,N'*-dialkyloxalamide (**6**), which was refluxed with phosphorus pentachloride in toluene to obtain dialkyloxalimide dichloride (**7**).[16f] Lithiated ethyl 2-thiopheneacetate was then combined with **7** at −78 °C and stirred at room temperature to afford a messy crude which after column chromatography gave the final product **5** in very low yield.

Next the isoDPPT acceptor unit was incorporated into copolymers using several donors as shown in Scheme 2.

Scheme 2. Synthesis of the Donor–Acceptor Copolymers by the Stille Coupling Reaction[a]
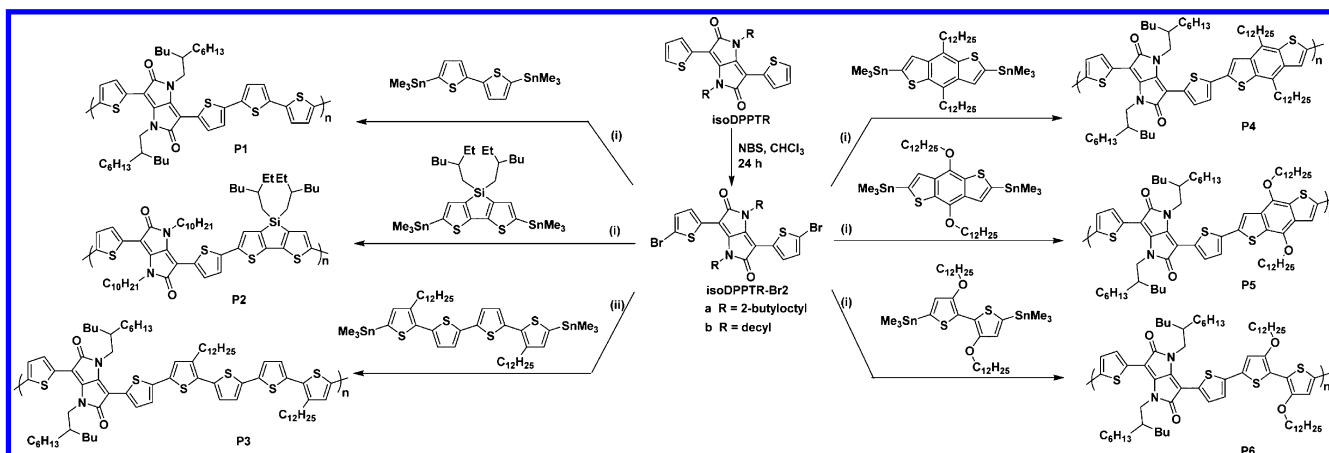
[a]Reaction conditions: (i) Pd$_2$(dba)$_3$, (o-Tol)$_3$P, toluene, 180 °C, MW, 5 h; (ii) Pd$_2$(dba)$_3$, (o-Tol)$_3$P, toluene, 130 °C, 44 h.

Table 1. Physical Properties [Molecular Weight[a] (M_w, KD), Polydispersity Index[a] (PDI), Optical Absorption Maximum (λ_{max}, nm) and Onset (λ_{onset}, nm), Optical Bandgap[b] (E_{op})], and Electrochemical Properties [Oxidation Onset[c] (E_{ox}), Reduction Onset[c] (E_{red}), Electrochemical Bandgap (E_{cv})]

			λ_{max}						
polymer	M_w	PDI	sol.	film	λ_{onset} film	E_{op}	E_{ox}	E_{red}	E_{cv}
P2	31.4	1.49	569	642	782	1.59	1.07	−0.92	1.99
P3	91.9	2.77	502	533	704	1.76	1.18	−0.95	2.13
P4	61.9	2.38	546	559	722	1.69	1.18	−0.96	2.14
P5	53.6	1.85	548	573	708	1.75	1.15	−0.96	2.11
P6	47.9	1.99	596	679	860	1.44	0.72	−1.04	1.76
P7[d]	31.1	2.8	798	796	963	1.29	0.34	−1.23	1.57
P8[d]	91.6	2.14	762	754	N.A.	1.45	0.77	−1.10	1.87

[a]M_w and PDI of the polymers were determined by high temperature gel permeation chromatography using polystyrene standards in trichlorobenzene at 150 °C. For representative plots see Figure S13, Supporting Information. [b]Calculated from the absorption band onsets of the copolymer films, E_g = 1240/ λ_{onset}. [c]Fc$^+$/Fc (0.54 V vs SCE) was used as internal reference for all measurements of polymer films on platinum electrode in acetonitrile solution containing 0.1 M Bu$_4$NPF$_6$ at a scan rate of 50 mV/s. E_{ox} and E_{red} are vs SCE. E_{cv} = E_{red} − E_{ox}. [d]References 12p and 12q while E_{ox} and E_{red} are vs Ag.
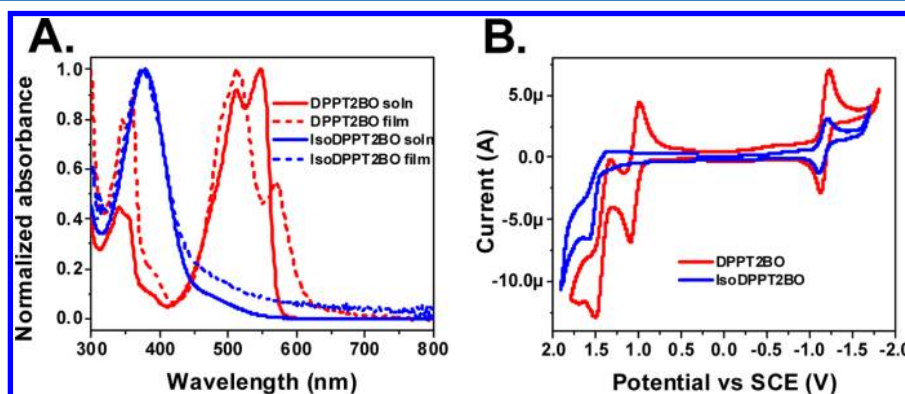

Figure 4. (A) Normalized absorption spectra of DPPT2BO and isoDPPT2BO in dichloromethane (DCM) solutions and in thin films. (B) Cyclic voltammograms of DPPT2BO and isoDPPT2BO in 0.1 M tetrabutylammonium hexafluorophosphate in dry DCM.

Synthetic details for these polymers can be found in the Experimental Section. Briefly, polymers **P1–P6** were prepared via Stille coupling by reacting isoDPPTR-Br$_2$ (prepared by bromination of isoDPPTR with NBS) with distannylated donor comonomers in toluene with Pd$_2$(dba)$_3$/o-Tol$_3$P as the catalyst using either a microwave reactor or a pressure vessel. **P1** was insoluble and no purification was attempted. The Soxhlet purified polymers **P2–P6** are soluble in chloroform and

chlorobenzene. Polymer molecular weights were determined by high temperature GPC versus polystyrene standards and found to be in the range from 30 kDa to 90 kDa with polydispersity index (PDI) of 1.5–2.8 (Table 1).

Optical and Electrochemical Properties. Optical absorption and electrochemical analysis (Figure 4) corroborate the dramatic changes of the electronic structure going from the DPPT to isoDPPT core, as suggested by the MO
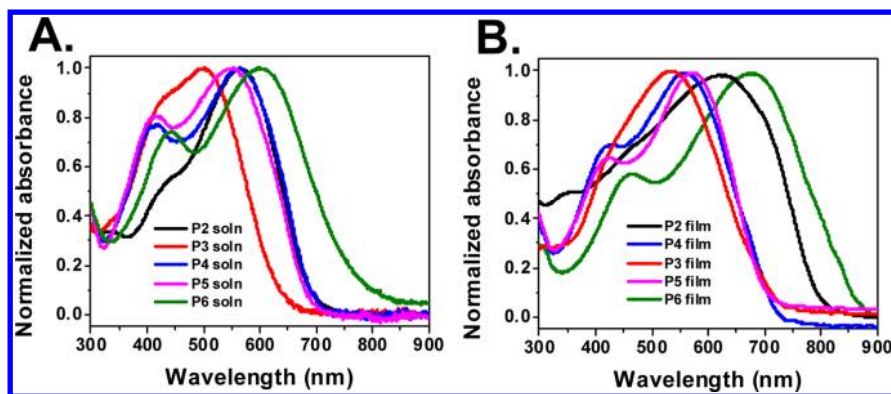
Figure 5. Normalized absorption spectra of polymers **P2**-**P6** (A) in chloroform solution and (B) as thin films.
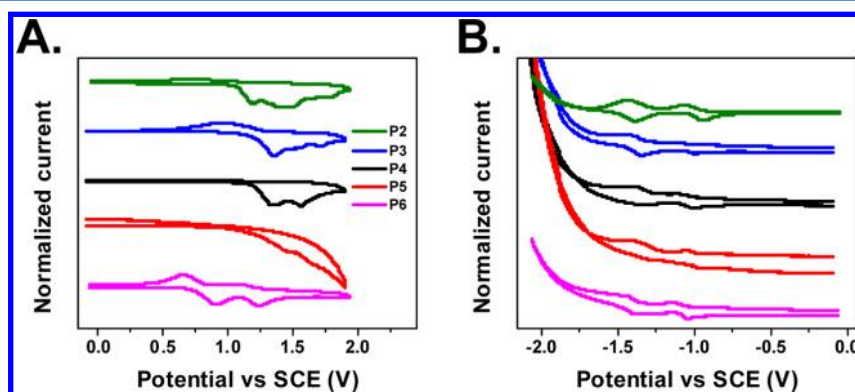

Figure 6. Cyclic voltammograms of **P2**−**P6** polymer thin films measured under nitrogen with 0.1 M tetra-*n*-butylammonium hexafluorophosphate in acetonitrile as the supporting electrolyte. (A) Oxidation curves and (B) reduction curves.

computations. Considering that the isoDPPT core is substantially planar in the solid state, these changes are primarily originating from the different bond connectivity and not due to conformational features of these two isomers. Indeed the maximum absorption of isoDPPT2BO (R = 2-butyloctyl, 2BO) in solution (film) is blue-shifted by ≈173 nm (≈ 196 nm) compared to DPPT2BO, resulting in a solution bandgap expansion from 2.17 to 2.77 eV (2.04 to 2.78 eV for thin-films). The absorption spectra of DPPT showed much finer vibronic features while isoDPPT2BO gave one broad absorption band with a long wavelength tail. The drastic deepening of the HOMO is confirmed by cyclic voltammetry, with the oxidation potential of isoDPPT2BO located at +1.45 V vs +1.05 V for DPPT2BO, whereas the reversible reduction waves are located at ≈ −1.2 V for both cores. Assuming the SCE energy level is −4.44 eV below the vacuum level, the estimated HOMO and LUMO energies are −5.89/−3.24 eV for isoDPPT2BO and −5.49/−3.24 eV for DPPT2BO, respectively. The very similar reduction potentials, and thus of their LUMO energy levels, are again consistent with the theoretical calculation results.

The optical properties of the isoDPPT-based polymers were also investigated by UV−vis absorption spectroscopy both in solution and as thin films (Figure 5). Relevant data are summarized in Table 1. To further rationalize the isoDPPT core and polymer properties, two DPPT-based polymers reported in the literature, PDPP-DTS (**P7**)[12p] and OH-D (**P8**)[12q] (Figure 1) having the same donors as **P2** and **P4**, respectively, are listed in these tables. All of the isoDPPT-based polymers exhibit strong absorption in the visible region with absorption maxima (λ_{max}) ranging from 502 to 596 nm in

solution and from 533 to 679 nm as thin films. From the absorption spectra, it can be seen that there are obvious bathochromic shifts on going from solution to the solid state, suggesting aggregation of these polymers promoted by previously observed core planarization of the isoDPPT monomer and intermolecular donor−acceptor interactions. The latter can be rationalized correlating the magnitude of the absorption maximum red shifts with the electron donating capacity for the various comonomers. Among these como-nomers, 3,3′-bis(dodecyloxy)-2,2′-bithiophene (for **P6**) has the largest electron density (donor strength), followed by 4,4′-bis(2-ethylhexyl)-dithieno[3,2-*b*:2′,3′-*d*]silole (for **P2**), 3,3‴-didodecylquaterthiophene (for **P3**), and benzo[1,2-*b*:4,5-*b*′]-dithiophene (for **P4** and **P5**) being the most electron-neutral. Indeed, the maximum bathochromic shift was observed for **P6** (83 nm), followed by **P2** (73 nm), **P3** (31 nm), **P4** (13 nm) and finally **P5** (25 nm). On the other hand, the absorption maximum of the DPPT analogues **P7** and **P8** undergoes a rather small blue shift (∼2 and 8 nm, respectively) strongly suggesting that no major conformational changes occur going from solution to the solid state and that these polymers are fairly rigid and already strongly aggregated in solution. The film optical bandgaps for the isoDPPT polymers derived from the absorption onsets fall within the range of 1.44 to 1.76 eV (Table 1), with the **P6** absorption extending into the near IR region. Compared to the isoDPPT polymers **P2** and **P4**, the corresponding DPPT polymers **P7** and **P8** exhibit much smaller optical bandgaps (0.30 and 0.24 eV, respectively), in agreement with the acceptor monomer computational and experimental results.

Table 2. HOMO (eV)[a], LUMO (eV)[a], OFET Characteristics [Charge Carrier Mobility (μ, cm^2/(V·s)), Current On/Off ratio (I_{on}:I_{off}) and Threshold Voltage (V_{th}, V)] and OPV Characteristics [Open Circuit Voltage (V_{oc}, V), Short Circuit Current Density (J_{sc}, mA/cm^2), Fill Factor (FF, %), and Power Conversion Efficiency (PCE, %)]

polymer	HOMO	LUMO	μ	I_{on}:I_{off}	V_{th}	V_{oc}	J_{sc}	FF	PCE
P2	−5.51	−3.52	3.4×10^{-2}	4×10^6	−12	0.76	10.28	65.0	5.1
P3	−5.62	−3.49	1.8×10^{-4}	1×10^5	−16	0.81	7.50	42.9	2.6
P4	−5.62	−3.48	4.3×10^{-4}	3×10^4	−24	0.88	9.91	42.1	3.7
P5	−5.59	−3.48	1.6×10^{-4}	2×10^5	−19	0.84	6.03	46.0	2.3
P6	−5.16	−3.40	2.5×10^{-4}	6×10^3	−3.2	0.44	1.60	43.0	0.3
P7[b]	−5.04	−3.47	N.A.	N.A.	N.A.	0.55	7.5	50.8	2.1
P8[c]	−5.15	−3.28	3.8×10^{-4}	41	−23.4	0.71	9.4	61	4.1

[a]HOMO = −(E^{ox} + 4.44) eV and LUMO = −(E^{red} +4.44) eV where E^{ox} and E^{red} are calculated vs SCE. [b]Reference 12p . [c]Reference 12q. Note that he HOMO and LUMO of OH-D (**P8**) were calculated with the quasi-reference electrode Ag/Ag$^+$ at 4.38 V while these of PDPP-DTS (**P7**) calculated with Ag/Ag$^+$ at 4.7 V.
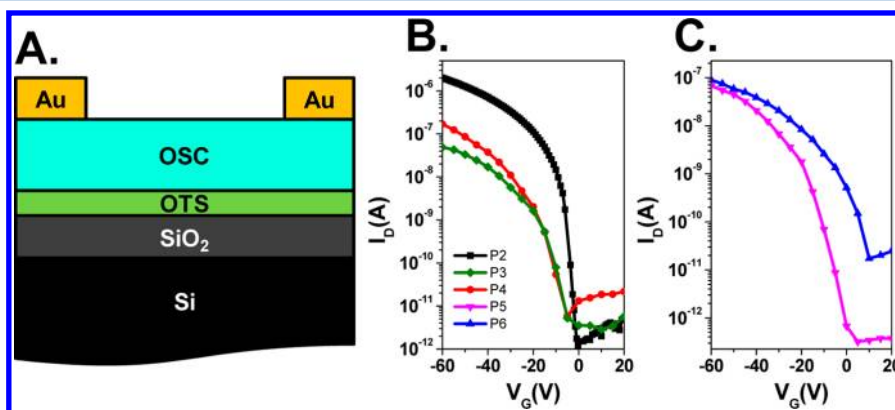

Figure 7. (A) Bottom-gate top-contact OTFT device structure. (B, C) Typical transfer curves of OTFT devices made of polymers **P2−P6**.
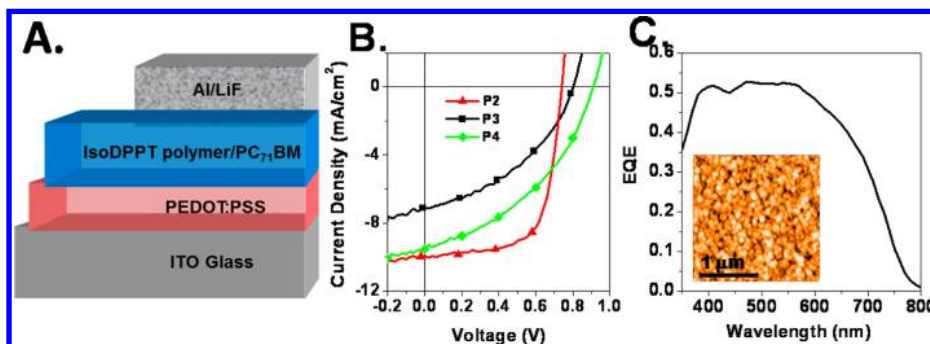

Figure 8. (A) Conventional organic bulk-heterojunction photovoltaic device structure. (B) J−V characteristic of OPV devices made of polymers **P2−P4** with PC$_{71}$BM as the active layers. (C) EQE measurements for polymer **P2** and (inset) AFM image of the corresponding **P2**:PC$_{71}$BM blend film.

The electrochemistry of the isoDPPT-based polymers **P2−P6** was investigated using thin-film cyclic voltammetry. The cyclic voltammograms of these polymers are shown in Figure 6, and relevant data are summarized in Table 2. All of the polymers show well-defined oxidation onsets and reversible reductions. On the basis of the reduction onsets, these polymers have rather similar LUMO energies (∼−3.5 eV), yielding LUMO−LUMO offsets with the PC$_{71}$BM acceptor of >0.3 eV, which should ensure efficient exciton dissociation.[23a] In contrast, their HOMO energies estimated from the corresponding oxidation onsets vary to a greater extent. The introduction of dialkoxybithiophene as the donor counit destabilized the HOMO of **P6**, resulting in the highest-lying HOMO of the series, −5.16 eV. However, polymers **P2−P5** exhibit closer HOMO energy levels falling from −5.51 to −5.62

eV. Note that the HOMO levels of **P2** and **P4** are considerably lower than those reported of the corresponding DPPT polymers **P7** (−5.04 eV) and **P8** (−5.15 eV), indicating that these isoDPPT polymers could have good oxidative stability and also enable high V_{oc} in bulk-heterojunction solar cells.

Thin-Film Transistor and Organic Photovoltaic Response. The charge transport properties of the new polymers were investigated by fabricating organic thin-film transistors (OTFTs, see Supporting Information). Bottom−gate top−contact OTFTs (Figure 7A) were fabricated on low resistivity n-type silicon wafers, using thermally grown SiO$_2$ (300 nm) passivated by octdecyltrichlorosilane (OTS) as the dielectric. Pristine polymer solutions (∼8 mg/mL in a solvent mixture of 97.5% chloroform and 2.5% dichlorobenzene by volume) were prepared, and the semiconductors were spun from solution

onto the substrates. The semiconductor films were then dried only at 120 °C for 5 min, an acceptable temperature in industry, without subsequent thermal annealing. Gold (Au) top-contacts (30 nm) were thermally evaporated through a shadow mask to complete the structure. All devices were characterized in ambient atmosphere and exhibited typical hole-transport properties (Figures 7B and 7C). Mobilities were calculated from saturation regimes and the average data (usually five devices were measured for each sample) are collected in Table 2 together with current modulation (I_{on}:I_{off}) and threshold voltages (V_{th}). These devices showed hole mobilities as high as 0.03 cm^2/(V·s) for polymer **P2** (I_{on}:I_{off} > 10^7, Vt ~ −10 V), whereas the mobilities of other polymers are lower, ranging ~10^{-4} cm^2/(V·s) (I_{on}:I_{off} ~ 10^4−10^5, V_t ~ −3 ~ −20 V), and comparable to those of the DPPT analogue **P8** (μ ~ 10^{-4} cm^2/(V·s), I_{on}:I_{off} ~ 10, V_t ~ −20 V). These metrics are far lower than the best, and highly crystalline, DPPT-based polymers. Indeed, WAXRD scans of the isoDPPT polymer films prepared under identical conditions used for TFT evaluation showed that even the best performing polymers are poorly crystalline (see Figure S11, Supporting Information for **P2** and **P4**). However, it is important to note that optimization of the DPPT copolymer structure, film microstructure, and thus FET performance involved extensive screening of donor monomers, solvents, dielectric surface treatment as well as thermal annealing of the semiconductor films.

Next, the photovoltaic performance of the present isoDPPT based polymers was investigated by fabricating conventional bulk-heterojunction (BHJ) solar cells having the following structure: ITO/PEDOT:PSS/polymer:PC$_{71}$BM/LiF/Al (Figure 8A, see the Supporting Information for device fabrication details). The active layers were prepared by spin-casting the polymer: PC$_{71}$BM blends with a 1:2 weight ratio from 9:1 chloroform:1,2-dichlorobenzene solutions and the blends were tested without postdeposition thermal annealing. The devices were characterized under a solar simulator at 100 mW/cm^2 simulated AM1.5G. The PV characteristics, including V_{oc}, short circuit current (J_{sc}), fill factor (FF) and power conversion efficiency (PCE) are summarized in Table 2. Representative J−V curves for **P2**-, **P3**-, and **P4**-based solar cells are presented in Figure 8B, as they perform better than those based on the other blends. Thus, the PCEs of the present iso-DPPT-based polymers, with the exception of **P6**, rank from ~2.3 to 5.1% with large V_{oc}'s ranging from 0.76 to 0.88 V. The FF values vary from respectable (65% for **P2**) to low (~42−46% for **P3**−**P5**). As expected, the **P6** polymer with very high HOMO exhibits far lower PCEs (~0.3%) as the result of the reduced photocurrent and much lower V_{oc} (0.44 V).

When comparing isoDPPT- (**P2** and **P4**) and DPPT-based (**P7** and **P8**) polymers with the same donor unit, the isoDPPT polymers exhibit larger V_{oc} (~0.2−0.3 V) as the result of the deeper HOMO energy levels and much larger (**P2** vs **P7**) or comparable (**P4** vs **P8**) PCE values. The best device performance is found for the **P2**-based solar cells with a J_{sc} = 10.28 mA/cm^2, V_{oc} = 0.76 V, FF = 65.0%, and PCE = 5.1%. The maximum EQE value for this device of ~50% is achieved in the region between 370 and 570 nm (Figure 8C). It is known that the morphology of the polymer/fullerene blend active layer plays a critical role in device performance.[23b] The active layer needs to provide continuous interpenetrating donor/acceptor domains for efficient charge carrier transport/collection at the respective electrodes and achieve nanoscale phase separation to maximize the exciton dissociation at the polymer/fullerene interface.[23c] Interestingly, AFM of these photoactive blends (Figure S12, Supporting Information) and of the **P2**/PC$_{71}$BM (Figure 8C, inset) indicate unoptimized thin-film morphologies characterized by oversized domains (>80−100 nm), which are much larger than the typical exciton diffusion length of ~20 nm.[23c] Thus, these morphologies are far from optimal, however, PSC metrics of **P2** and **P4** without intensive optimization are still comparable/larger than those of the structurally similar DPPT polymers **P7** and **P8**, showing the potential of isoDPPT as a promising acceptor building block for organic optoelectronics.

CONCLUSIONS

The acceptor building block 3,6-dithiophen-2-yl-diketopyrrolo-[3,2-b]pyrrole (isoDPPT) has been designed, synthesized, and investigated by molecular orbital computations, optical spectroscopy, electrochemistry, and single crystal X-ray diffraction. Interesting structural details and evidence of large conformational changes from solution to the solid state for isoDPPTR vs conventional DPPTR derivatives were presented as well as insights into the origin of the lower HOMO energy of this core. Then isoDPPT was incorporated as an acceptor building block with several typical donor comonomers to realize the new polymers **P1** − **P6**. OTFT and OPV devices based on these polymers were fabricated and investigated. Among this series, polymer **P2** exhibit the greatest performance with hole mobilities of ~0.03 cm^2/(V·s) in ambient and OPV PCEs >5%, for active films without thermal treatment. We strongly believe that optimization of isoDPPT-based polymers from the materials chemistry community will further validate the potential of this building block for opto-electronic device applications as currently are the excellent DPPT-based polymers.

ASSOCIATED CONTENT

ⓢ Supporting Information

^{1}H NMR spectra of compounds **1−5**, isoDPPTDec-Br2, and isoDPPT2BO-Br2, fabrication details of OTFT and OPV devices, representative GPC plots, and single crystal data collection and refinement with selected bond lengths and angles. This material is available free of charge via the Internet at http://pubs.acs.org.

AUTHOR INFORMATION

Corresponding Author

*E-mail: slu@polyera.com (S.L.); a-facchetti@northwestern.edu (A.F.).

Notes

The authors declare no competing financial interest.

REFERENCES

(1) (a) Seri, M.; Marrocchi, A.; Bagnis, D.; Ponce, R.; Taticchi, A.; Marks, T. J.; Facchetti, A. *Adv. Mater.* **2011**, *23*, 3827. (b) Ortiz, R. P.; Herrera, H.; Seoane, C.; Segura, J. L.; Facchetti, A.; Marks, T. J. *Chem.—Eur. J.* **2012**, *18*, 532. (c) Feng, L.; Rudolf, M.; Wolfrum, S.; Troeger, A.; Slanina, Z.; Akasaka, T.; Nagase, S.; Martin, N.; Ameri, T.; Brabec, C. J. *J. Am. Chem. Soc.* **2012**, *134*, 12190. (d) Osaka, I.; Shimawaki, M.; Mori, H.; Doi, I.; Miyazaki, E.; Koganezawa, T.; Takimiya, K. *J. Am. Chem. Soc.* **2012**, *134*, 3498. (e) McCulloch, I.; Ashraf, R. S.; Biniek, L.; Bronstein, H.; Combe, C.; Donaghey, J. E.; James, D. I.; Nielsen, C. B.; Schroeder, B. C.; Zhang, W. *Acc. Chem. Res.* **2012**, *45*, 714. (f) Djukic, B.; Perepichka, D. F. *Chem. Commun.* **2012**, *48*, 6651. (g) Beverina, L.; Ruffo, R.; Salamone, M. M.; Ronchi,

E.; Binda, M.; Natali, D.; Sampietro, M.; Pagani, G. A. *J. Mater. Chem.* **2012**, *22*, 6704. (h) Lv, A.; Puniredd, S. R.; Zhang, J.; Li, Z.; Zhu, H.; Jiang, L.; Li, Y.; Pisula, W.; Meng, Q.; Hu, W.; Wang, Z. *Adv. Mater.* **2012**, *24*, 2626. (i) Facchetti, A. *Chem. Mater.* **2010**, *23*, 733. (j) Henson, Z. B.; Müllen, K.; Bazan, G. C. *Nature Chem.* **2012**, *4*, 699. (k) Beverina, L.; Drees, M.; Facchetti, A.; Salamone, M.; Ruffo, R.; Pagani, G. A. *J. Org. Chem.* **2011**, *28*, 5555. (l) Bagnis, D.; Beverina, L.; Huang, H.; Silvestri, F.; Yao, Y.; Yan, H.; Pagani, G. A.; Marks, T. J.; Facchetti, A. *J. Am. Chem. Soc.* **2010**, *132*, 4074.

(2) (a) Sciascia, C.; Martino, N.; Schuettfort, T.; Watts, B.; Grancini, G.; Antognazza, M. R.; Zavelani-Rossi, M.; McNeill, C. R.; Caironi, M. *Adv. Mater.* **2011**, *23*, 5086. (b) Wang, C.; Dong, H.; Hu, W.; Liu, Y.; Zhu, D. *Chem. Rev.* **2012**, *112*, 2208. (c) Chabinyc, M. L.; Salleo, A. *Chem. Mater.* **2004**, *16*, 4509. (d) Melucci, M.; Zambianchi, M.; Favaretto, L.; Gazzano, M.; Zanelli, A.; Monari, M.; Capelli, R.; Troisi, S.; Toffanini, S.; Muccini, M. *Chem. Commun.* **2011**, *47*, 11840. (e) Generali, G.; Dinelli, F.; Capelli, R.; Toffanin, S.; Muccini, M. *J. Phys. D: Appl. Phys.* **2011**, *44*, 224018. (f) Peters, C. H.; Sachs-Quintana, I. T.; Mateker, W. R.; Heumueller, T.; Rivnay, J.; Noriega, R.; Beiley, Z. M.; Hoke, E. T.; Salleo, A.; McGehee, M. D. *Adv. Mater.* **2012**, *24*, 663. (g) Dacuna, J.; Salleo, A. *Phys. Rev. B* **2011**, *84*, 195209. (h) Salleo, A.; Kline, R. J.; DeLongchamp, D. M.; Chabinyc, M. L. *Adv. Mater.* **2010**, *22*, 3812. (i) Rivnay, J.; Toney, M. F.; Zheng, Y.; Kauvar, I. V.; Chen, Z.; Wagner, V.; Facchetti, A.; Salleo, A. *Adv. Mater.* **2010**, *22*, 4359. (j) Tsumura, A.; Koezuka, H.; Ando, T. *Appl. Phys. Lett.* **1986**, *49*, 1210.

(3) (a) Baeg, K.-J.; Khim, D.; Jung, S.-W.; Kang, M.; You, I.-K.; Kim, D.-Y.; Facchetti, A.; Noh, Y.-Y. *Adv. Mater.* **2012**, *24*, 5433. (b) Wang, C.; Dong, H.; Hu, W.; Liu, Y.; Zhu, D. *Chem. Rev.* **2012**, *112*, 2208. (b) Beaujuge, P. M.; Fréchet, J. M. J. *J. Am. Chem. Soc.* **2011**, *133*, 20009. (c) Tsao, H. N.; Cho, D. M.; Park, I.; Hansen, M. R.; Mavrinskiy, A.; Yoon, D. Y.; Graf, R.; Pisula, W.; Spiess, H. W.; Müllen, K. *J. Am. Chem. Soc.* **2011**, *133*, 2605.

(4) (a) Li, Y. *Acc. Chem. Res.* **2012**, *45*, 723. (b) Zhang, Z.-G.; Wang, J. *J. Mater. Chem.* **2012**, *22*, 4178. (c) Zhou, H.; Yang, L.; You, W. *Macromolecules* **2012**, *45*, 607. (d) Li, G.; Zhu, R.; Yang, Y. *Nature Photon.* **2012**, *6*, 153. (e) Brabec, C. J.; Gowrisanker, S.; Halls, J. J. M.; Laird, D.; Jia, S.; Williams, S. P. *Adv. Mater.* **2010**, *22*, 3839. (f) Arias, A. C.; MacKenzie, J. D.; McCulloch, I.; Rivnay, J.; Salleo, A. *Chem. Rev.* **2010**, *110*, 3. (g) Cheng, Y.-J.; Yang, S.-H.; Hsu, C.-S. *Chem. Rev.* **2009**, *109*, 5868. (h) Chen, J.; Cao, Y. *Acc. Chem. Res.* **2009**, *42*, 1709. (i) Takacs, C. J.; Sun, Y.; Welch, G. C.; Perez, L. A.; Liu, X.; Wen, W.; Bazan, G. C.; Heeger, A. J. *J. Am. Chem. Soc.* **2012**, *134*, 16597. (j) Shirman, T.; Freeman, D.; Shimon, L.; Feldman, I.; Van Der Boom, M.; Facchetti, A. *J. Am. Chem. Soc.* **2008**, *130*, 8162.

(5) (a) Davis, A. R.; Maegerlein, J. A.; Carter, K. R. *J. Am. Chem. Soc.* **2011**, *133*, 20546. (b) Kamtekar, K. T.; Monkman, A. P.; Bryce, M. R. *Adv. Mater.* **2010**, *22*, 572.

(6) (a) Brown, A. R.; Pomp, A.; de Leeuw, D. M.; Klaassen, D. B. M.; Havinga, E. E.; Herwig, P.; Müllen, K. *J. Appl. Phys.* **1996**, *79*, 2136. (b) Afzali, A.; Dimitrakopoulos, C. D.; Breen, T. L. *J. Am. Chem. Soc.* **2002**, *124*, 8812. (c) Anthony, J. E.; Brooks, J. S.; Eaton, D. L.; Parkin, S. R. *J. Am. Chem. Soc.* **2001**, *123*, 9482.

(7) (a) Halik, M.; Klauk, H.; Zschieschang, U.; Schmid, G.; Radlik, W.; Ponomarenko, S.; Kirchmeyer, S.; Weber, W. *Adv. Mater.* **2003**, *13*, 197. (b) Garnier, F.; Yassar, A.; Hajlaoui, R.; Horowitz, G.; Deloffre, F.; Servet, B.; Ries, S.; Alnot, P. *J. Am. Chem. Soc.* **1993**, *115*, 8716. (c) Wu, X.; Chen, T.-A.; Rieke, R. D. *Macromolecules* **1995**, *28*, 2101. (d) Loewe, R. S.; McCullough, R. D. *Polym. Prepr.* **1999**, *40*, 852. (e) Sirringhaus, H.; Brown, P. J.; Friend, R. H.; Nielsen, M. M.; Bechgaard, K.; Langeveld-Voss, B. M. W.; Spiering, A. J. H.; Janssen, R. A. J.; Meijer, E. W.; Herwig, P.; de Leeuw, D. M. *Nature* **1999**, *401*, 685. (f) Ong, B. S.; Wu, Y.; Liu, P.; Gardner, S. *J. Am. Chem. Soc.* **2004**, *126*, 3378. (g) Ma, W.; Yang, C.; Gong, X.; Lee, K.; Heeger, A. J. *Adv. Funct. Mater.* **2005**, *15*, 1617.

(8) (a) Laquindanum, G.; Katz, H. E.; Lovinger, A. J. *J. Am. Chem. Soc.* **1998**, *120*, 664. (b) McCulloch, I.; Heeney, M.; Bailey, C.; Genevicius, K.; Macdonald, I.; Shkunov, M.; Sparrowe, D.; Tierney, S.; Wagner, R.; Zhang, W.; Chabinyc, M. L.; Kline, R. J.; McGehee, M. D.;

Toney, M. F. *Nat. Mater.* **2006**, *5*, 328. (c) Wu, Y.; Li, Y.; Gardner, S.; Ong, B. S. *J. Am. Chem. Soc.* **2005**, *127*, 614. (d) Kazuo, T.; Shoji, S.; Itaru, O.; Eigo, M. *Adv. Mater.* **2011**, *23*, 43477.

(9) (a) Zhan, X.; Facchetti, A.; Barlow, S.; Marks, T. J.; Ratner, M. A.; Wasielewski, M. R.; Marder, S. R. *Adv. Mater.* **2011**, *23*, 268. (b) Huo, L.; Hou, J. *Polym. Chem.* **2011**, *2*, 2453. (c) Liang, Y.; Yu, L. *Acc. Chem. Res.* **2010**, *43*, 1227. (d) Boudreault, P. T.; Beaupre, S.; Leclerc, M. *Polym. Chem.* **2010**, *1*, 127. (e) Ohshita, J. *Macromol. Chem. Physic.* **2009**, *210*, 1360. (f)

(10) Bürgi, L.; Turbiez, M.; Pfeiffer, R.; Bienewald, F.; Kimer, H.-J.; Winnewisser, C. *Adv. Mater.* **2008**, *20*, 2217.

(11) Wienk, M. M.; Turbiez, M.; Gilot, J.; Janssen, R. A. J. *Adv. Mater.* **2008**, *20*, 2556.

(12) For selected reviews, see (a) Tieke, B.; Rabindranath, A. R.; Zhang, K.; Zhu, Y. *Beilstein J. Org. Chem.* **2010**, *6*, 830. (b) Qu, S.; Tian, H. *Chem. Commun.* **2012**, *48*, 3039. (c) Nielsen, C. B.; Turbiez, M.; McCulloch, I. *Adv. Mater.* **2012**, *25*, 1859. For selected recent publication on OTFTs, see: (d) Chen, H.; Guo, Y.; Yu, G.; Zhao, Y.; Zhang, J.; Gao, D.; Liu, H.; Liu, Y. *Adv. Mater.* **2012**, *24*, 4618. (e) Lee, J. S.; Son, S. K.; Song, S.; Kim, H.; Lee, D. R.; Kim, K.; Ko, M. J.; Choi, D. H.; Kim, B.; Cho, J. H. *Chem. Mater.* **2012**, *24*, 1316. (f) Lin, H.-W.; Lee, W.-Y.; Chen, W.-C. *J. Mater. Chem.* **2012**, *22*, 2120. (g) Chen, Z.; Lee, M. J.; Ashraf, R. S.; Gu, Y.; Albert-Seifried, S.; Nielsen, M. M.; Schroeder, B.; Anthopoulos, T. D.; Heeney, M.; McCulloch, I.; Sirringhaus, H. *Adv. Mater.* **2012**, *24*, 647. (h) Ha, J. S.; Kim, K. H.; Choi, D. H. *J. Am. Chem. Soc.* **2011**, *133*, 10364. (i) Li, Y.; Sonar, P.; Singh, S. P.; Soh, M. S.; van Meurs, M.; Tan, Z. *J. Am. Chem. Soc.* **2011**, *133*, 2198. (j) Kanimozhi, C.; Yaacobi-Gross, N.; Chou, K. W.; Amassian, A.; Anthopoulos, T. D.; Patil, S. *J. Am. Chem. Soc.* **2012**, *134*, 16532. For selected recent publication on OPVs, see: (k) Liu, F.; Gu, Y.; Wang, C.; Zhao, W.; Chen, D.; Briseno, A. L.; Russell, T. P. *Adv. Mater.* **2012**, *24*, 3947. (l) Jung, J. W.; Jo, J. W.; Liu, F.; Russell, T. P.; Jo, W. H. *Chem. Commun.* **2012**, *48*, 6933. (m) Bijleveld, J. C.; Zoombelt, A. P.; Mathijssen, S. G. J.; Wienk, M. M.; Turbiez, M.; de Leeuw, D. M.; Janssen, R. A. J. *J. Am. Chem. Soc.* **2009**, *131*, 16616. (n) Dou, L.; Gao, J.; Richard, E.; You, J.; Chen, C.-C.; Cha, K. C.; He, Y.; Li, G.; Yang, Y. *J. Am. Chem. Soc.* **2012**, *134*, 10071. (o) Bijleveld, J. C.; Gevaerts, V. S.; Nuzzo, D. D.; Turbiez, M.; Mathijssen, S. G. J.; de Leeuw, D. M.; Wienk, M. M.; Janssen, R. A. J. *Adv. Mater.* **2010**, *22*, E242. (p) Huo, L.; Hou, J.; Chen, H.-Y.; Zhang, S.; Jiang, Y.; Chen, T. L.; Yang, Y. *Macromolecules* **2009**, *42*, 6564. (q) Li, Z.; Zhang, Y.; Tsang, S.-W.; Du, X.; Zhou, J.; Tao, Y.; Ding, J. *J. Phys. Chem. C* **2011**, *115*, 18002. (r) Dou, L.; Gao, J.; Richard, E.; You, J.; Chen, C.-C.; Cha, K. C.; He, Y.; Li, G.; Yang, Y. *J. Am. Chem. Soc.* **2012**, *134*, 10071.

(13) (a) Qiao, Y.; Guo, Y.; Yu, C.; Zhang, F.; Xu, W.; Liu, Y.; Zhu, D. *J. Am. Chem. Soc.* **2012**, *134*, 4084. (b) Zhang, Y.; Kim, C.; Lin, J.; Nguyen, T.-Q. *Adv. Funct. Mater.* **2012**, *22*, 97. (c) Tantiwiwat, M.; Tamayo, A.; Luu, N.; Dang, X.-D.; Nguyen, T.-Q. *J. Phys. Chem. C* **2008**, *112*, 17402.

(14) (a) Walker, B.; Tamayo, A. B.; Dang, X.-D.; Zalar, P.; Seo, J. H.; Garcia, A.; Tantiwiwat, M.; Nguyen, T.-Q. *Adv. Funct. Mater.* **2009**, *19*, 3063. (b) Lee, O. P.; Yiu, A. T.; Beaujuge, P. M.; Woo, C. H.; Holcombe, T. W.; Millstone, J. E.; Douglas, J. D.; Chen, M. S.; Fréchet, J. M. *Adv. Mater.* **2011**, *23*, 5359. (c) Loser, S.; Bruns, C. J.; Miyauchi, H.; Ortiz, P.; Facchetti, A.; Stupp, S.; Marks, T. J. *J. Am. Chem. Soc.* **2011**, *133*, 8142.

(15) (a) Lu, S.; Facchetti, A.; Yao, Y.; Drees, M.; Yan, H. US2011/0226338, 2011. (b) *N,N′*-diaryl isoDPPT based conjugated copolymers were recernly reported without any application in organoelectronics. See: Welterlich, I.; Chaov, O.; Tieke, B. *Macromolecules* **2012**, *45*, 4511. (c) During the preparation of our manuscript, a copolymer of *N,N′*-diaryl isoDPPT with *N*-alkylated carbazole was published giving hole mobility of 2.2×10^{-5} cm^2/(V·s) in bottom gate top contact devices and PCEs of up to 2.0%. See: Song, S.; Ko, S.-J.; Shin, H.; Jin, Y.; Kim, I.; Kim, J. Y.; Suh, H. *Syn. Met.* **2012**, 2288. (d) Very recently the synthesis and optical properties of isoDPP-oligothiophenes were reported. See: Kirkus, M.; Knippenberg, S.; Beljonne, D.; Cornil, J.; Janssen, R. A. J.; Meskers, S. C. J. *J. Phys. Chem. A* **2013**, *117*, 2782.

(16) (a) Hou, J.; Chen, H.-Y.; Zhang, S.; Li, G.; Yang, Y. *J. Am. Chem. Soc.* **2008**, *130*, 16144. (b) Yue, W.; Zhao, Y.; Tian, H.; Song, D.; Xie, Z.; Yan, D.; Geng, Y.; Wang, F. *Macromolecules* **2009**, *42*, 6510. (c) Zhu, Z.; Drees, M.; Pan, H.; Yao, Y.; Yan, H.; Lu, S.; Facchetti, A. US2010/135701, 2010. (d) Hou, J.; Park, M.-H.; Zhang, S.; Yao, Y.; Chen, L.-M.; Li, J.-H.; Yang, Y. *Macromolecules* **2008**, *41*, 6012. (e) Watson, M. D. US2010/0252112, 2010. (f) Janietz, S.; Barche, J.; Wedel, A.; Sainova, D. *Macromol. Chem. Phys.* **2004**, *205*, 1916.

(17) *Spartan'08*; Wavefunction, Inc.: Irvine, CA, 2008.

(18) Luňák, S.; Vyňuchal, J.; Hrdina, R. *J. Mol. Struct.* **2009**, *919*, 239.

(19) Naik, M.; Kanimozhi, C.; Nutalapati, V.; Patil, S. *J. Phys. Chem. C* **2012**, *116*, 26128.

(20) Fürstenwerth, H. Ger. Offen. DE 3525109 A1, 1987.

(21) (a) Solberg, Y. Z. *Naturforsch.* **1977**, *32c*, 292. (b) Rochat, A. C.; Iqbal, A.; Pfenninger, J.; Casser, L. Eur. Pat. Appl. EP 0163609 A2, 1984.

(22) (a) Helmholz, F.; Schroeder, R.; Langer, P. *Synthesis* **2006**, 2507. (b) Langer, P.; Helmholz, F.; Schroeder, R. *Synlett* **2003**, 2389. (c) Langer, P.; Wuckelt, J.; Döring, M. *J. Org. Chem.* **2000**, *65*, 729. (d) Wuckelt, J.; Döring, M.; Langer, P.; Görls, H.; Beckert, R. *Tetrahedron Lett.* **1997**, *38*, 5269.

(23) (a) Scharber, M. C.; Mühlbacher, D.; Koppe, M.; Denk, P.; Waldauf, C.; Heeger, A. J.; Brabec, C. J. *Adv. Mater.* **2006**, *18*, 789. (b) Peet, J.; Heeger, A. J.; Bazan, G. C. *Acc. Chem. Res.* **2009**, *42*, 1700. (c) Coakley, K. M.; McGehee, M. D. *Chem. Mater.* **2004**, *16*, 4533.